KEK ACCELERATORS AND FUTURE PROJECTS

Toshio SUZUKI

National Laboratory for High Energy Physics
Oho-machi, Tsukuba-gun, Ibaraki-ken, 300-32, Japan

Abstract

The constructional and working aspects of the KEK 12 GeV proton synchrotron are described. Then, we outline the Photon Factory project, which is a dedicated synchrotron radiation source facility now under construction. Finally, we explain the TRISTAN project which is an electron-proton colliding beam machine project now under detailed design study.

§1. Introduction

KEK is an institute established in 1971 with the 12 GeV proton synchrotron as its main facility. The construction of the proton synchrotron started in 1971 and completed in 1976. The physics experiments using the proton beam started in 1977. Now, we have achieved the design energy and intensity of 12 GeV and 2×10^{12} ppp (protons per pulse). Still, much effort is being made to improve the intensity and beam characteristics of the machine. In 1976, a project started to utilize the 500 MeV booster beam for pulsed-neutron diffraction experiments, π-μ physics experiments, medical and biological applications etc.

In 1977, a new project started in KEK. It is the Photon Factory project which is a combination of a 2.5 GeV electron linac and a 2.5 GeV electron storage ring aimed at a dedicated synchrotron radiation source. The design study of the machine was formerly in progress at the Institute for Nuclear Study (INS), University of Tokyo and KEK. The construction of this machine is expected to be completed in 1981.

We are now working on the design of the TRISTAN project as a future extension of the present 12 GeV proton synchrotron and the 2.5 GeV Photon Factory electron linac. It is a project to construct an electron-proton colliding beam machine of 20 GeV electrons and 300 GeV protons. Since such a new machine requires many technical developments, we are now working on the developments of the superconducting magnet system, the ultra-high vacuum system etc, in addition to the design study of the machine.

In this short talk, we outline the design, constructional and working aspects of the 12 GeV proton synchrotron, the Photon Factory synchrotron radiation source and the TRISTAN project. Since the time is limited, we only describe the essential features of the machines. For

the detailed description of the principles of accelerator physics, the reader is referred to the references cited at the end of this note.

§2. General Description of the 12 GeV Proton Synchrotron

Fig.1 shows the layout of the accelerators in the KEK site which has an area of 1 Km × 2 Km. Only the 12 GeV P.S. (Proton Synchrotron) is now under operation. The 2.5 GeV electron linac and the electron storage ring are now under construction. The TRISTAN ring is a future project now under design study. The 200 MeV high intensity electron linac and the 3 GeV stacking ring are designed for positron stacking in the TRISTAN ring.

Fig.2 shows the layout of the 12 GeV proton synchrotron complex. It consists of four separate accelerators; the 750 keV preinjector, the 20 MeV linac, the 500 MeV booster synchrotron and the 12 GeV proton synchrotron (main ring). The protons ionized in the ion source are accelerated by these four accelerators, fast extracted for bubble chamber experiemnts and slow extracted for counter experiments. Extraction using an internal target is also used for counter experiments. A part of the beam from the 500 MeV booster, which is not used for injection into the main ring, is shared by pulsed magnets and used for the facilities utilizing the booster beam.

The average radius (circumference divided by 2π) of the booster is 6 m and that of the main ring is 54 m. Since the circumference of the main ring is nine times larger than that of the booster, it requires nine booster acceleration cycles to fill the main ring with protons as shown in Fig.2. The time sequence of the accelerators is shown in Fig.3. The repetition rate of the booster synchrotron is chosen to be 20 Hz, and the injectors, i.e. the preinjector and the linac are accordingly

operated at 20 Hz. Since nine booster beam pulses are injected into the main ring, it takes about 0.5 sec for beam injection into the main ring. During injection, the magnetic field of the main ring is held constant. Then, as the beam is accelerated, the magnetic field rises and again becomes flat for beam extraction. The magnetic field then decreases to the injection field. The magnetic field is about 1.5 kG at the injection energy of 500 MeV and about 17.5 kG at 12 GeV. The cycle time of the main ring is 2 sec. Since only nine booster pulses are necessary to fill the main ring, the other eleven pulses are used for the booster beam facilities and for the linac beam measurement.

More detailed time sequence up to the booster is shown in Fig.4. The booster magnetic field changes sinusoidally with the injection field of about 2 kG and the maximum field of about 11 kG. The linac beam pulses are injected during about 10 μsec. The revolution time of the proton beam in the booster at 20 MeV is 1.5 μsec so that the linac pulses are injected during about seven turns.

Fig.5 shows a photograph of the main ring intensity. We see that the intensity goes up step by step at injection while nine booster pulses are injected. The intensity is almost flat during acceleration with a small loss at transition energy (which will be explaiend in §6) and decreases as the beam is extracted. In the same figure, the traces of the magnetic field and the extracted beam intensity are also shown. The maximum intensity in the main ring achieved so far is 2.3×10^{12} protons per pulse.

§3. Preinjector and Beam Transport System

Fig.6 shows the preinjector. It is a high voltage DC accelerator. A high voltage of 750 kV is applied to the accelerating column shown

at the left of the figure. Protons emerging from an ion source are accelerated by a DC potential. Quadrupole magnets are installed in the accelerating column to ensure transverse focusing. The high voltage is generated by a Cockcroft-Walton type high voltage generator shown at the right of the figure. It essentially consists of rectifiers and capacitors, and in one stage, a DC potential which is twice as high as the applied AC potential is obtained. Since the generator consists of four stages, the DC potential at the top of the generator is eight times as high as the applied AC voltage. Note that the applied AC voltage of 80 kV denotes an effective voltage and that its amplitude is 113 kV.

Fig.7 shows the ion source. The hydrogen gas from a gas bombe is ionized by the electrons emitted from the heated cathode and forms a proton-electron plasma. The protons are extracted electrostatically by the electrodes. The plasma is confined in a small region by the geometrical configuration of the electrodes and by the longitudinal magnetic field produced by a solenoid. Since this type of ion source has a dual focusing fuction, it is called a "duoplasmatron".

Focusing of charged particles is very important in accelerators. There are two methods of focusing. The first one is the focusing by solenoids shown in Fig.8. Charged particles are trapped in the magnetic field and does not diverge. The focusing force is rather weak compared to the second method of focusing by quadrupole magnets and, in high energy accelerators, the quadrupole magnets are mainly used for focusing.

The quadrupole magnet is shown in Fig.9. It consists of four poles which have a hyperbolic profile. The magnetic field is zero at the center and increases linearly with the distance from the center, i.e. the field "gradient" is constant. In Fig.9, the force exerted on protons is such that it is focusing vertically and defocusing horizontally. The

reverse focusing is obtained by reversing the current flowing through the coils of the magnet. Since the quadrupole magnet is focusing in one direction and defocusing in the other, it is necessary to combine a horizontally focusing (F) magnet and a horizontally defocusing (D) magnet as shown at the right of Fig.9 to obtain net focusing.

Quadrupole magnets are much used in beam transport systems. Fig.10 shows the low energy beam trasnport system between the preinjector and the linac. In this system, a quadrupole quadruplet (a combination of four quadrupoles) and five quadrupole triplets (a combination of three quadrupoles) are used to achieve focusing. The quadrupole strengths are so adjusted that the beam shape in phase space (emittance) from the preinjector is matched to the shape (acceptance) which is accepted by the linac. Fig.11 shows a beam transport system between the linac and the booster. In this system, twenty-three quadrupole magnets are used.

§4. Linear Accelerator (Linac)

The 20 MeV linear accelerator (linac) is shown in Fig.12. The main constituents of the linac are the resonator tank (cavity), in which a standing wave electromagnetic field is excited, and the drift tubes which shield the electromagnetic field and through which the proton beam passes. The frequency of the electromagnetic wave is 200 MHz. Since the frequency lies in the range usually used in radio applications, the high frequency electromagnetic wave used in high energy accelerators is called an RF (radio frequency) wave.

The RF power is fed from the outside source by way of the two feed lines as shown in the figure. The mode of the electromagnetic wave is a so-called TM_{010}-mode which has a longitudinal electric field component used for acceleration. The drift tubes are metallic tubes which shield

the electromagnetic field so that the beam does not receive any force when it is inside the drift tubes. The beam receives an accelerating force in the gaps between the drift tubes when the electric field is in the accelerating direction. When the electric field is in the wrong direction, the beam is inside the drift tube and receives no decelerating force. The length of the drift tubes increases as the energy and accordingly the velocity of the protons increases. The total length of the linac tank is about 16 m and the diameter of the tank is about 0.9 m.

Stability of longitudinal motion (phase stability) is very important in understanding the operation of the linac. The beam must pass through the gaps between the drift tubes when the electric field is rising as shown at the left of Fig.13. The particle having a right energy determined by the length of the drift tubes is made to pass at a certain fixed phase of the RF voltage called a synchronous phase angle ϕ_s and that particle is called a synchronous particle. The particles having an energy larger than the synchronous particle travels with a greater velocity and passes through the next gap ahead of the synchronous particle. The particles then receive less electric field since the field is rising and the energy gain becomes less. Thus, the particles initially having a larger energy tend to be accelerated less. The opposite holds for particles having a lower energy. Thus, the particles oscillate in energy and phase around the synchronous energy and phase (phase oscillation or synchrotron oscillation, since this fact was first found in connection with synchrotrons) and phase stability is assured. Phase stability breaks down if the particles pass through the gaps when the electric field is falling.

The condition of phase stability makes the transverse motion unstable. This is seen with reference to the right of Fig.13. The electric field

in the gap is bent inward as shown in the figure. At time t_1, the protons receive a focusing force and at time t_2, they receive a defocusing force. Since the field is rising, the defocusing force is greater and we get transverse instability. In order to compensate this defocusing force of RF, we install small quadrupole magnets inside the drift tubes as shown in the figure.

§5. Booster Synchrotron

The 500 MeV booster shown in Fig.14 is a circular accelerator called a synchrotron. The beam is confined in a circular orbit by bending magnets, and the beam energy is slowly increased by an RF cavity while the beam revolves many turns. The momentum p of a particle expressed in GeV/c is related to the bending field B expressed in Tesla (1 Tesla = 10 kG) and the radius of curvature ρ expressed in m by the following relation,

$$p\ (\mathrm{GeV/c}) = 0.3\ B\ (\mathrm{Tesla})\ \rho\ (\mathrm{m}). \qquad (1)$$

As the energy increases, the bending field increases correspondingly to fix the radius of curvature constant. The maximum energy gain per revolution in the booster is 7 keV. The RF frequency ranges from 1.6 MHz at injection to 6.0 MHz at 500 MeV to fit the revolution frequnecy of the beam.

The whole circumference is divided into eight identical sections called cells or periods, and each cell consists of a magnet ($M_1 \sim M_8$) and a field-free straight section ($S_1 \sim S_8$). The straight sections are used to install equipments for beam injection (injection septum magents and injection bump magnets), equipments for beam ejection (ejection

septum magnets, an ejection kicker magnet, ejection bump magnets), RF-cavities, beam position monitors (Pos), intensity monitors ($I_1 \sim I_8$), profile monitors (Pr) and other auxiliary equipments.

The particle having a right momentum and injected at right angle and position travels in a circular path, but most other particles will be lost unless means are provided to focus the beam. Longitudinal stability is obtaied by accelerating the beam in the rising part of RF, quite similarly to the phase stability explained in the section on the linac. The transition energy to be explained in connection with the main ring is 1.23 GeV and well above the maximum energy of 500 MeV.

Transverse stability is achieved by using magnets as shown in Fig.15. The magnet has a pole shape which is a part of a hyperbola and, in addition to the bending field, it has a constant field gradient and thus a focusing power. It can be considered to be a part of a displaced quadrupole magnet. It has a horizontally focusing (F) property or a horizontally defocusing (D) property. By combining F and D magnets we obtain focusing action in both horizontal and vertical directions. Since the type of magnet has a bending as well as focusing property, it is called a "combined-function" type magnet. Another focusing scheme is a "separated function" type focusing employed in the main ring which uses dipole magnets having a flat pole shape as a bending unit and quadrupole magnets as a focusing element.

The particles injected at wrong angle and position with respect to an equilibirum orbit (the orbit on which travels a particle injected with right momentum, angle and position) oscillate stably about the equilibrium orbit due to the focusing action of the magnets. This oscillation is called "betatron oscillation" since it is first analyzed in detail with respect to an accelerator called a betatron. The number of betatron

oscillations per revolution is called a "tune" and it plays an important role in synchrotrons. An integral or half-integral tune is dangerous and should be avoided because it leads to a dangerous linear resonance and thus to beam loss. The tune is chosen to be 2.2 horizontally and 2.3 vertically in the booster.

§6. Main Ring

Fig.16 shows the layout of the main ring and Fig.17 shows its lattice structure. It is a synchrotron having an average radius of 54 m and a bending radius of 24.6 m. There are cells called normal cells which consist of two quadrupole magnets and two bending magnets and cells forming a long straight section in which one bending magnet is removed from the normal cell. Five normal cells ($N_3 \sim N_7$) and two long straight section cells (L_1, L_2) form a superperiod and there are four superperiods in the main ring. The four long straight sections are used for beam injection, installing RF cavities, fast extraction for bubble chamber experiments and slow extraction for counter experiments. One of the short straight sections is used for an internal target beam as shown in Fig.16. The focusing scheme of the main ring is a separated function type focusing which uses dipole bending magnets for bending and quadrupole magnets for focusing. The cross section of the magnets is shown in Fig.18.

Phase stability of the main ring is somewhat complicated due to the presence of transition energy. We consider phase stability of the circular machine in some detail. In circular machines in contrast to linear machines like a linac, the factor determining phase stability is not a linear velocity v, but rather an angular velocity ω. v and ω are related by

$$\omega = \frac{v}{R}, \tag{2}$$

where R is the average radius (circumference divided by 2π) of the machine. A small change in ω due to small change in momentum p is expressed as

$$\frac{\Delta\omega}{\omega} = \frac{\Delta v}{v} - \frac{\Delta R}{R}$$

$$= \left(\frac{1}{\gamma^2} - \frac{1}{\gamma_t^2} \right) \frac{\Delta p}{p}, \tag{3}$$

where the relations

$$\frac{\Delta v}{v} = \frac{1}{\gamma^2} \frac{\Delta p}{p} \tag{4}$$

$$\frac{\Delta R}{R} = \alpha \frac{\Delta p}{p} = \frac{1}{\gamma_t^2} \frac{\Delta p}{p}, \tag{5}$$

are used. Eq.(4) is a usual relativistic kinematical relation, where γ is a Lorentz factor. Eq.(5) is a relation which is determined by the lattice structure (the way of arranging magnets). The momentum compaction factor α or the transition-γ, γ_t, is a constant determined by the lattice structure alone. By looking at eq.(3), we see that $\Delta\omega > 0$ when $\gamma < \gamma_t$, i.e. the particle having a larger momentum revolves faster, but that $\Delta\omega < 0$ when $\gamma > \gamma_t$, i.e. the particle having a larger momentum revolves slower above the transition energy. The transition energy is usually expressed by the kinetic energy or $m_0c^2(\gamma_t - 1)$ where m_0c^2 is the rest mass energy of the particle. It is about 5.4 GeV in the main ring. Phase stability below and above transition energy is explained in Fig.19. The mechanism is similar to the one encountered in the linac case.

We only replace the linear velocity by the angular velocity. Below transition, phase stability is achieved by accelerating particles in the rising part of the RF wave, whereas above transiton, the particles should be accelerated in the falling side of the RF wave. At transiton, the phase of RF should be switched by $180°-2\phi_s$ in a short time of the order of 100 μsec. Instability is likely to occur at transtion and there is some beam loss at transition as shown in Fig.5.

At the maximum operating energy, the beam is extracted fastly or slowly. The principle of fast shaving extraction is simple as shown in Fig.20. The beam is displaced by bump magnets towards an electric septum in which an intense electrostatic field of 60 kV/cm is applied. The particles which enter the septum are deflected and extracted, while the other particles receive no force and circulate in the machine as before. The beam is thus extracted in a time interval of the order of μsec. (The revolution time is about 1.1 μsec.)

In slow resonant extraction, the beam is extracted slowly in a time interval of 500 msec. The process uses a nonlinear resonance of betatron oscillations. The horizontal tune is moved towards a half-integral value where half-integral resonance is excited and particles become unstable. By use of an octupole magnet in this case, it is possible to make those particles having a small oscillation amplitude stable and to make only the particles having large oscillation amplitudes unstable as shown in Fig.20. The unstable particles rapidly go outside and inside alternately by steps of two turns, jump into the septum and become extracted. As the tune becomes closer to a half-integral value, the stable region shrinks. It is therefore the essential point of the resonant slow extraction to finely control the tune and to move the tune to a half-integral value as slowly and smoothly as possible. Fig.21

shows the stable regions and the motion of unstable particles (denoted by dots) expressed in the phase space diagram (x: horizontal coordinate, x': horizontal angle).

§7. Photon Factory Storage Ring

The Photon Factory is a facility dedicated for synchrotron light source. The electrons passing through a bending magnet are accelerated by a centripetal force and emit x-rays called synchrotron radiation as shown in Fig.22. The rms emission angle $\sqrt{\langle\theta^2\rangle}$ is nearly equal to $1/\gamma$ and is extremely small, where γ is a Lorentz factor. The x-rays are used for various experimental purposes. The spectrum of synchrotron radiation is shown in Fig.23. The energy of the storage ring is 2.5 GeV and the bending field is 1 Tesla (= 10 kG). The wavelength is in the Å range. In a straight section high field superconducting magnets of 6 Tesla called wigglers are added. Then the wavelength goes to down to 0.1 Å range.

The lattice structure of the storage ring is shown in Fig.24. The storage ring has a race - track shape and has two long straight sections. The average radius is 28.4 m and the bending radius is 8.33 m. The lattice is of a separated-function type. It has 28 bending magnets and 58 quadrupole magnets.

The electrons are injected from the 2.5 GeV linac repetitively and 500 mA of current (1.9×10^{12} electrons) is stored in the ring. The injection system consists of the four kicker magnets (K1 ∿ K4) and two septum magnets (S1, S2). The energy loss due to synchrotron radiation is compensated by RF cavities.

The injection linac is a travelling wave type linac in contrast to the standing wave structure of the proton linac. The electromagnetic

wave travels in the linac tank with the velocity of light and the electrons travel with the same speed as the electromagentic wave while lying on the crest of the wave as shown in Fig.25. In a simple wave-guide structure, the phase velocity of the electromagnetic wave is generally greater than the velocity of light. So, the disks are inserted in the wave-guide as shown in Fig.26 in order to slow down the phase velocity of the wave to the velocity of light.

The energy of the linac is 2.5 GeV and its peak current is 50 mA in 10 μsec pulse length. The linac is operated with a repetition rate of 50 Hz. The RF frequency is 2856 MHz.

§8. TRISTAN Project

The TRISTAN project is a project to construct a colliding beam machine of 20 GeV electrons and 300 GeV protons. As an option, an electron-positron colliding beam machine of 25 GeV in each energy is envisaged. The electron-proton colliding beam machine has a center-of-mass energy of 155 GeV and corresponds to an ordinary accelerator of 12.8 TeV.

Luminosity L is an important quantity in storage rings. It is defined by the relation

$$Y(\mathrm{sec}^{-1}) = L(\mathrm{cm}^{-2}\mathrm{sec}^{-1})\sigma(\mathrm{cm}^{2}), \qquad (6)$$

where Y is the yield expressed in sec^{-1}, σ is the cross section expressed in cm^2 and luminosity L is expressed in unit of $\mathrm{cm}^2\mathrm{sec}^{-1}$. The luminosity proposed for TRISTAN is 3×10^{31} $\mathrm{cm}^{-2}\mathrm{sec}^{-1}$ for electron-proton collision and 1×10^{32} $\mathrm{cm}^{-2}\mathrm{sec}^{-1}$ for electron-positron collision. The luminosity for electron-proton collision is achieved by 14 A of protons (7.7×10^{14} protons) and 200 mA of electrons (1.1×10^{13} electrons).

The layout of the TRISTAN rings is shown in Fig.27. TRISTAN consists of three rings, Rings I, II and III. Ring I is an electron or positron storage ring. The injector is the Photon Factory linac. Ring II is a proton booster ring which accelerates protons from 12 GeV to 50 GeV. The injector is the 12 GeV proton synchrotron. Ring III is a proton storage ring made of superconducting magnets. The protons from Ring II are injected and accelerated to 300 GeV. The colliding region has a magnet-free space of 20 m. The total length of the straight section is 150 m. The ring has four intersecting regions.

The average radius of the TRISTAN rings is 420 m. The bending radius of the three rings differs slightly from ring to ring and lies in the range of 220 to 250 m. The maximum bending field of the superconducting magnets is 4.5 Tesla.

We hope that the construction of TRISTAN will start in 1982 and will be completed in 1988.

Acknowledgement

Many figures in this note are taken from various KEK publications. Especially, many figures are taken from Y. Kimura, "KEK 12 GeV Proton Synchrotron" in "Proc. 1976 KEK Summer School (ref.4)". We thank these authors for making the figures available.

References

1. H. Kumagai (ed.): "Kasokki" in "Jikken - Butsurigaku - Koza, vol.28", Kyoritsu Shuppan (1975).
2. M.S. Livingston and J.P. Blewett: "Particle Accelerators", McGraw-Hill (1962).
3. S. Flüge (ed.): "Nuclear Instrumentation I" in "Handbuch der Physik vol XLIIV", Springer Verlag (1959).

4. Proc. 1976 KEK Summer School, KEK-76-10 (1976).
5. G. Horikoshi (ed.): "Lecture Notes on the Physics and Technology of the KEK Proton Synchrotron (in Japanese)" KEK-77-20 (1978).

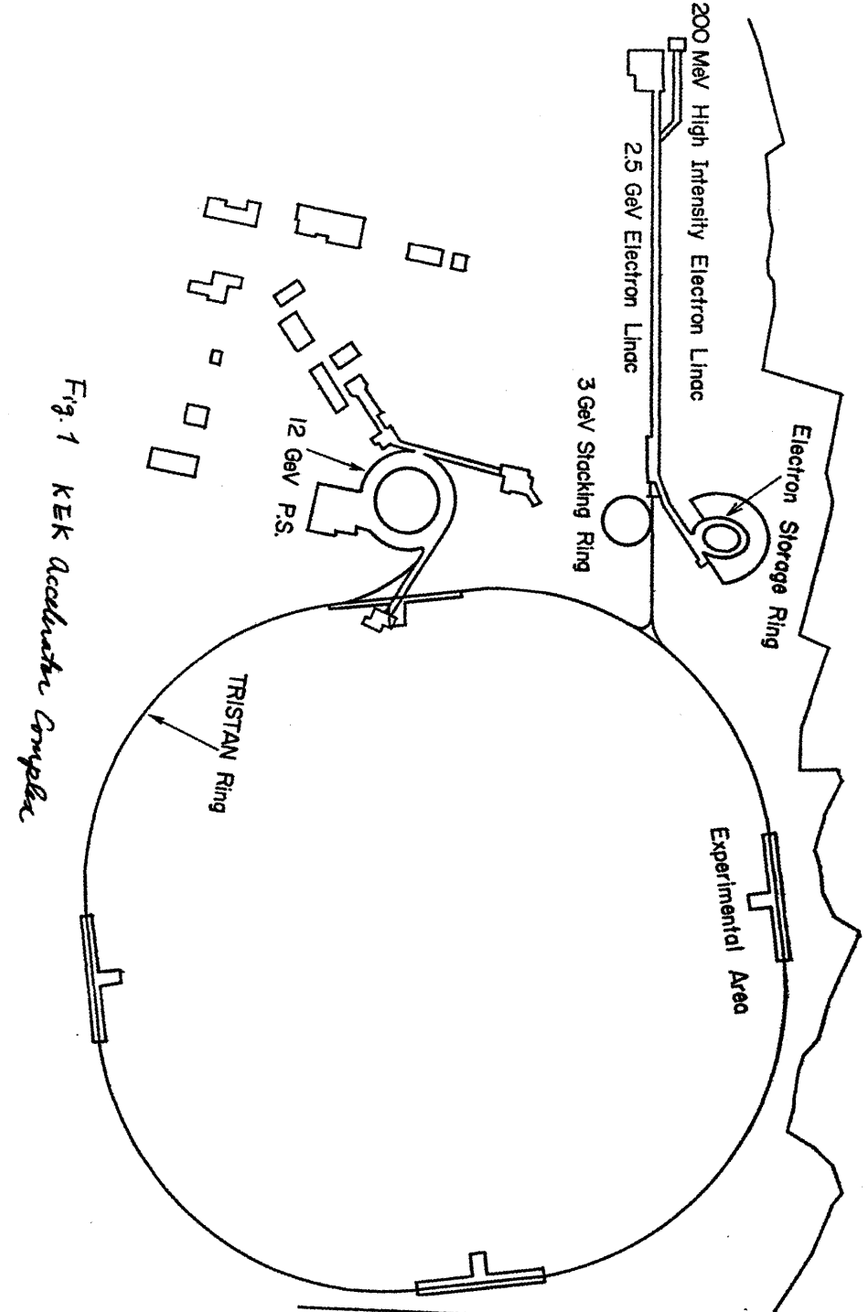

Fig. 1 KEK accelerator complex

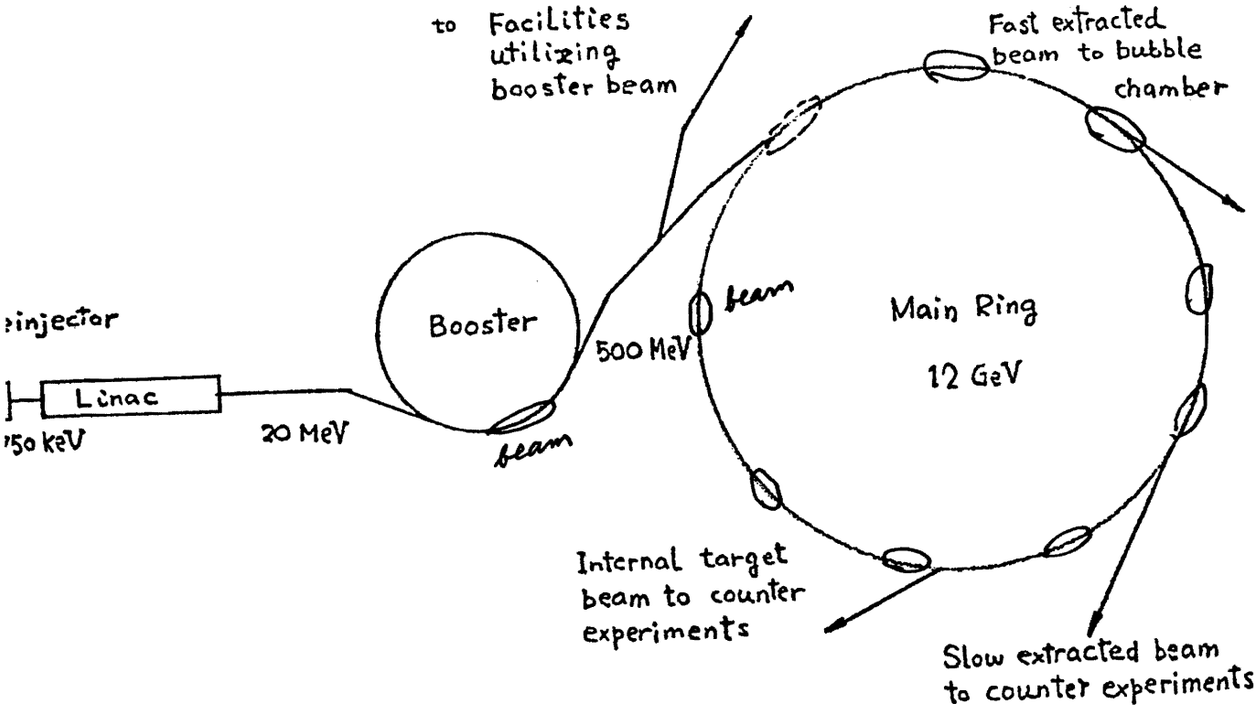

Fig. 2 12 GeV Proton Synchrotron

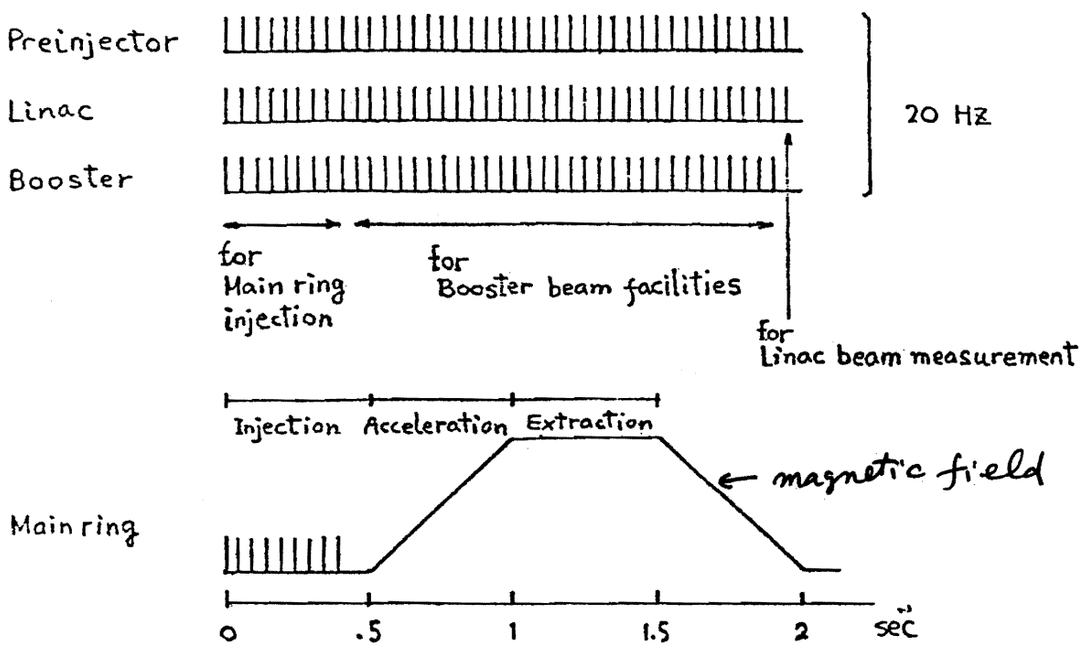

Fig. 3 Time sequence of the 12 GeV Proton Synchrotron

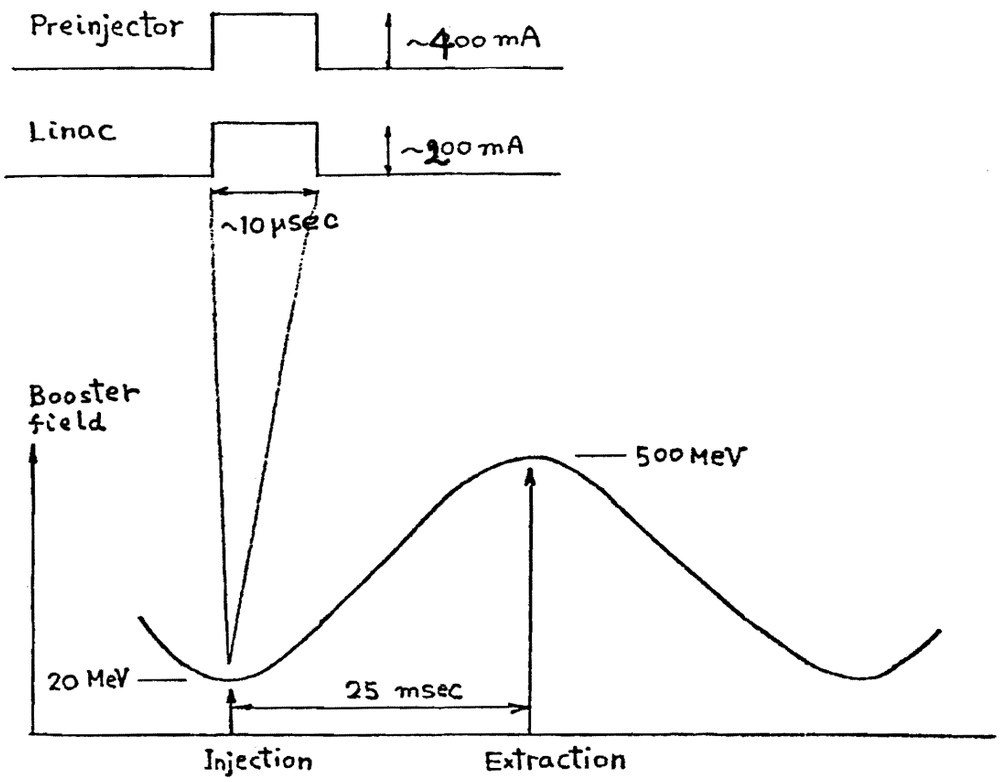

Fig.4 Time sequence up to Booster

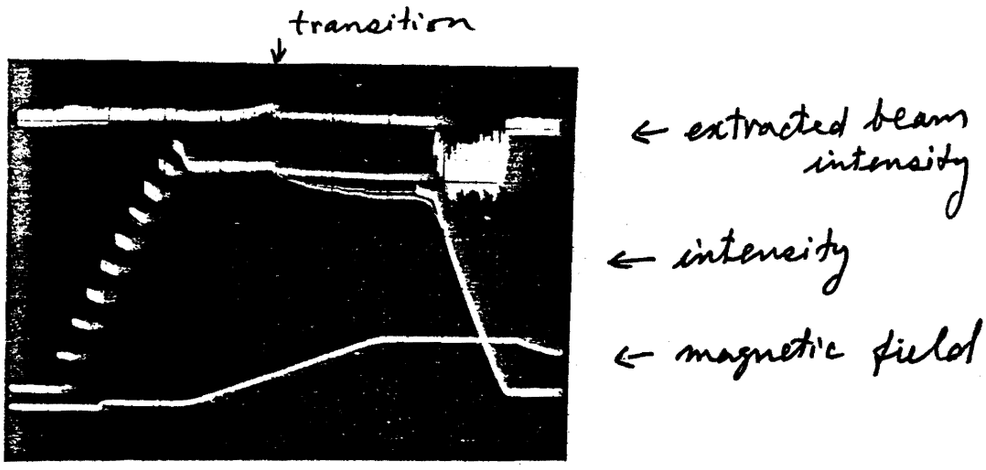

Fig.5 main ring intensity

Fig. 6 Preinjector

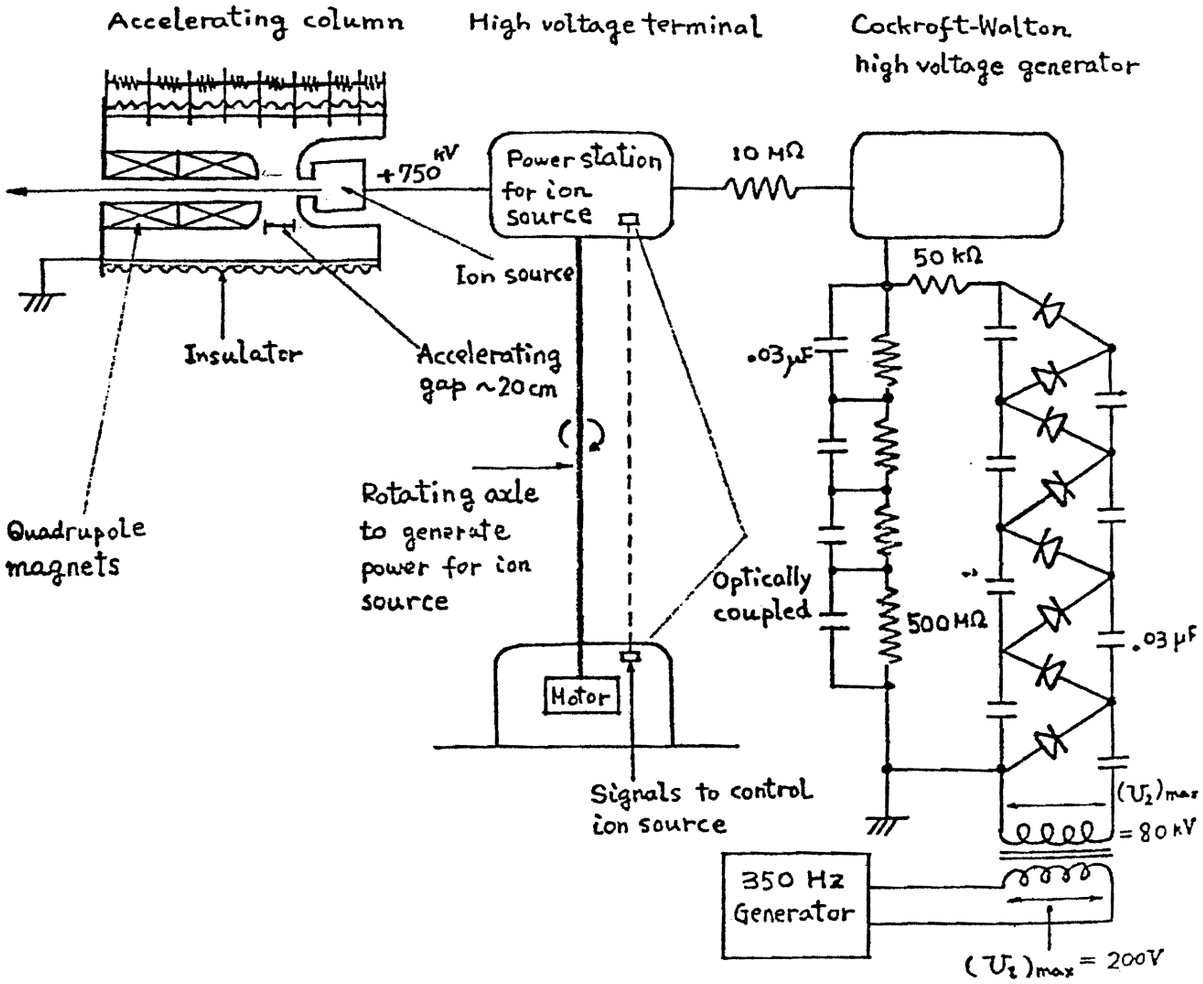

Fig. 7 Ion source

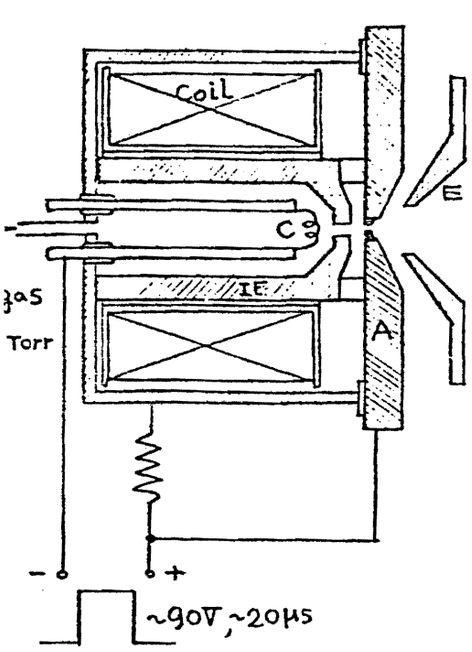

Fig. 5

Ion source

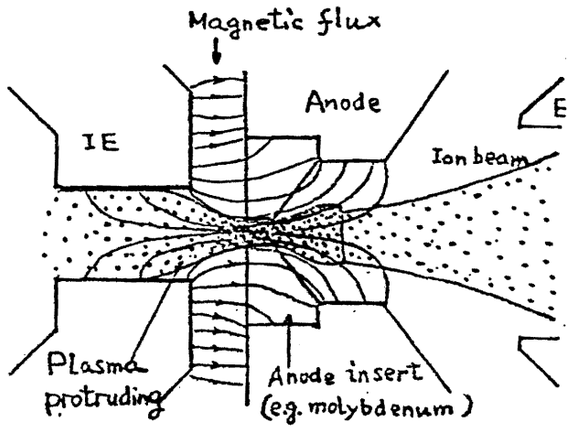

C – Heated cathode

IE – Intermediate electrode (steel)

A – Anode (steel)

E – Extractor electrode (stainless steel)

□ – Insulator

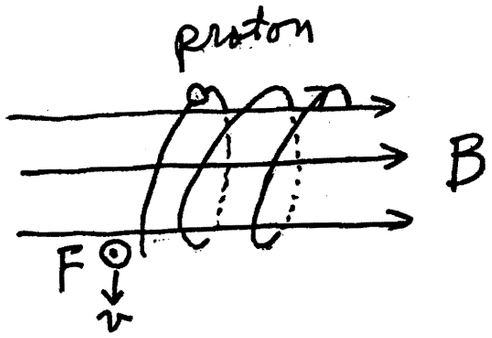

Fig. 8 Focusing by Solenoid

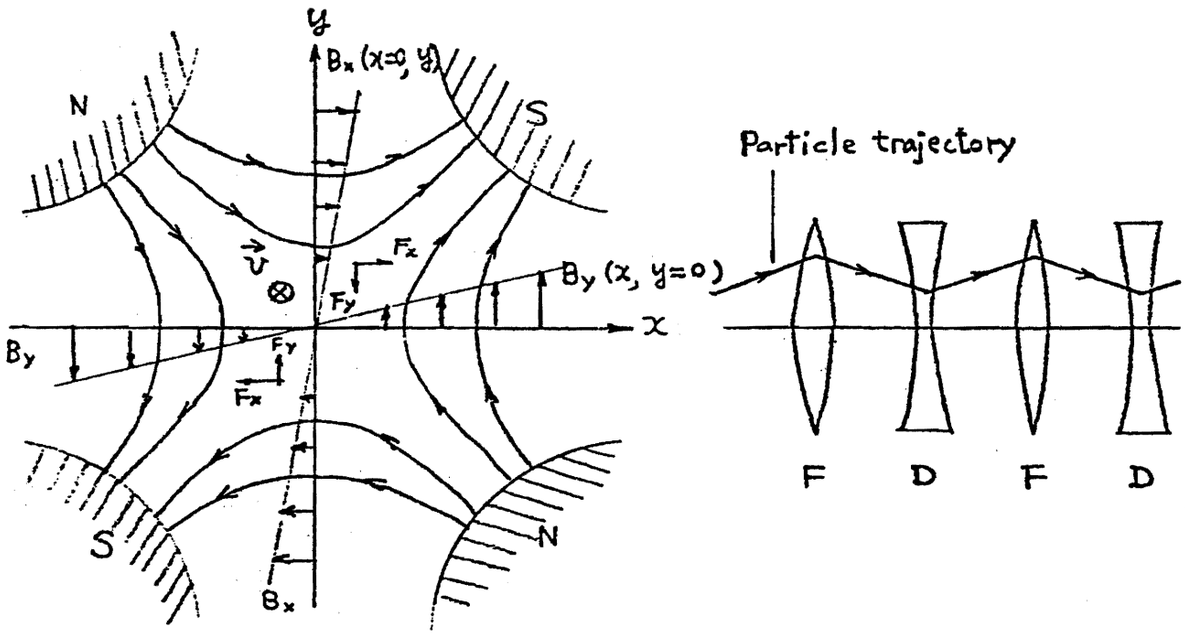

Fig. 9 Focusing by Quadrupole magnet

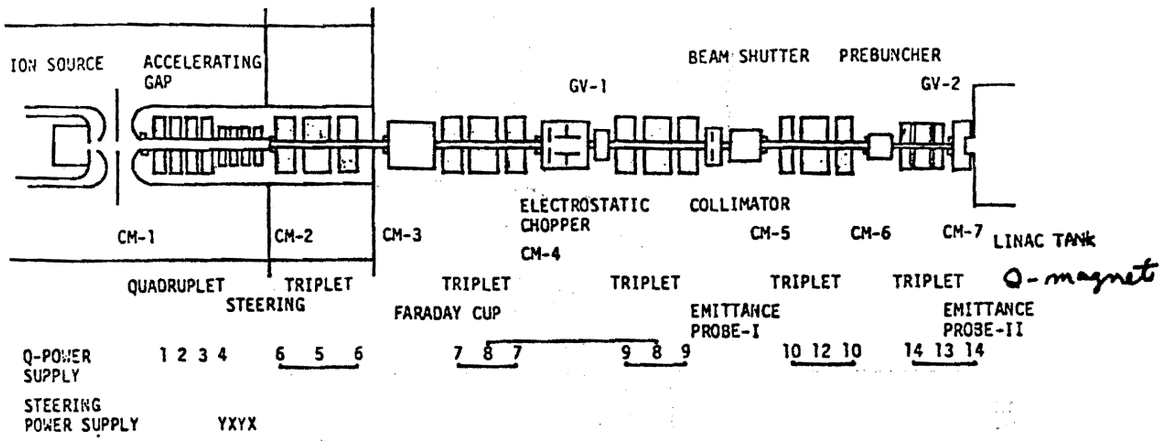

Fig. 10 Low Energy Beam Transport (LEBT)

Preinjector → Linac

Fig. 11 BEAM TRANSPORT LINE BETWEEN LINAC AND BOOSTER

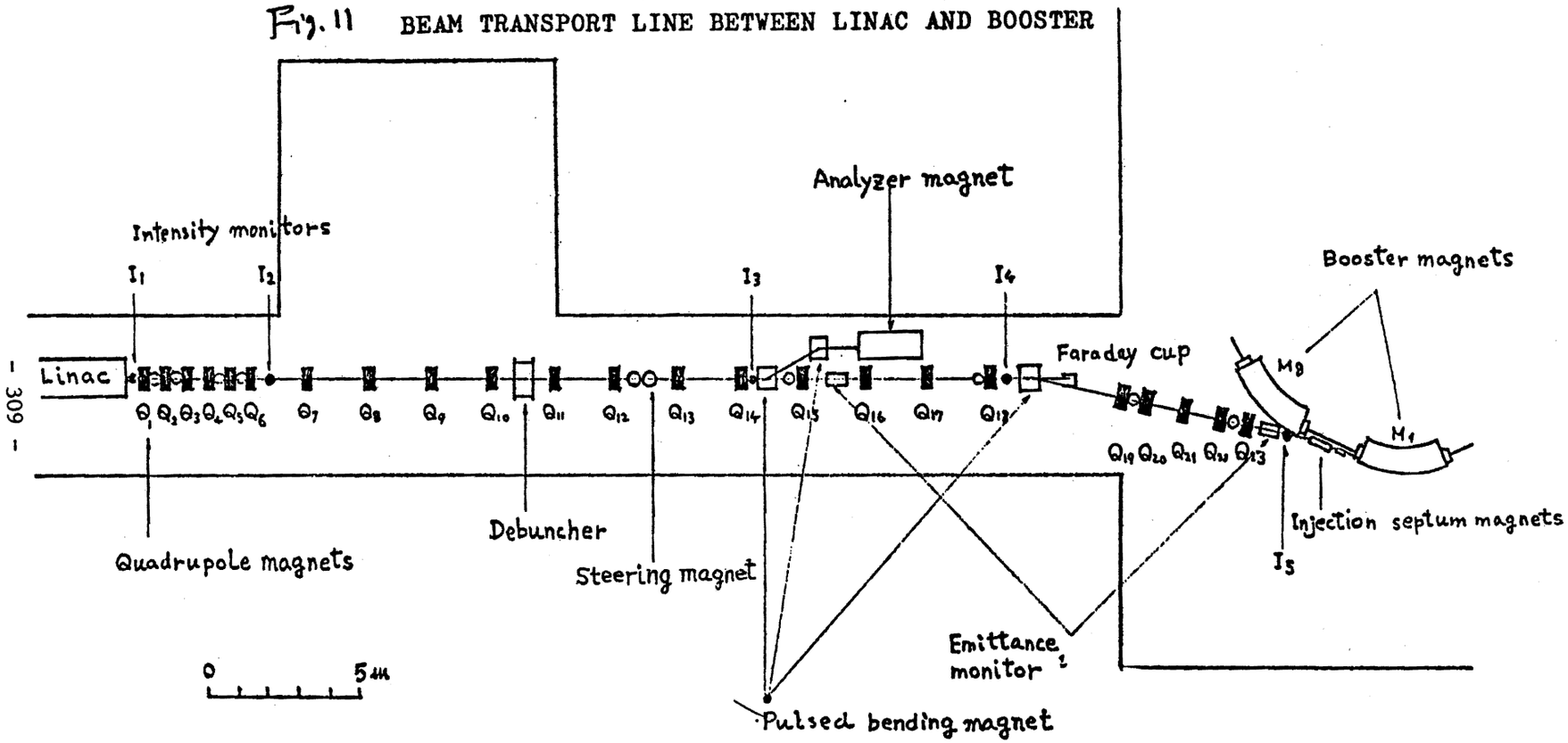

Fig. 12 20MeV Linac

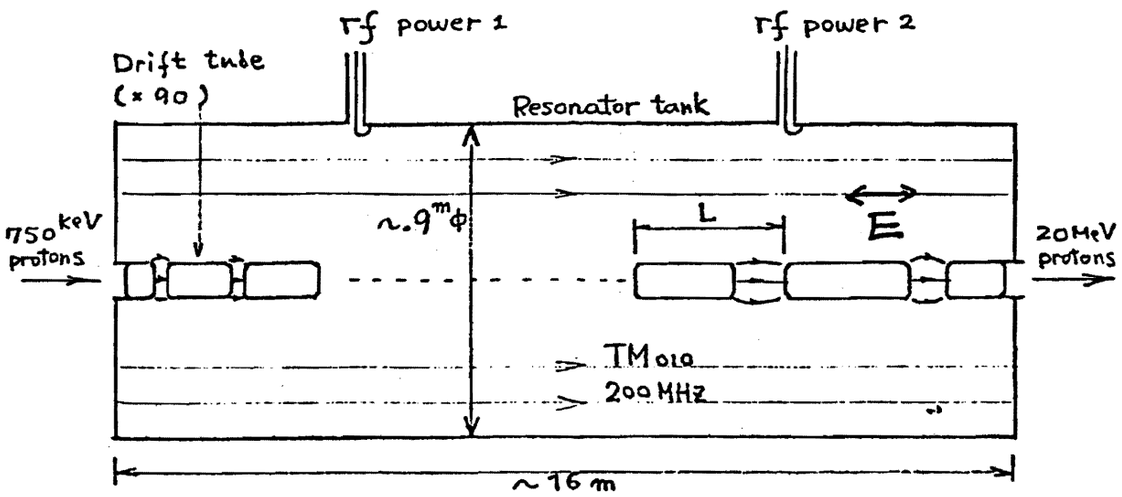

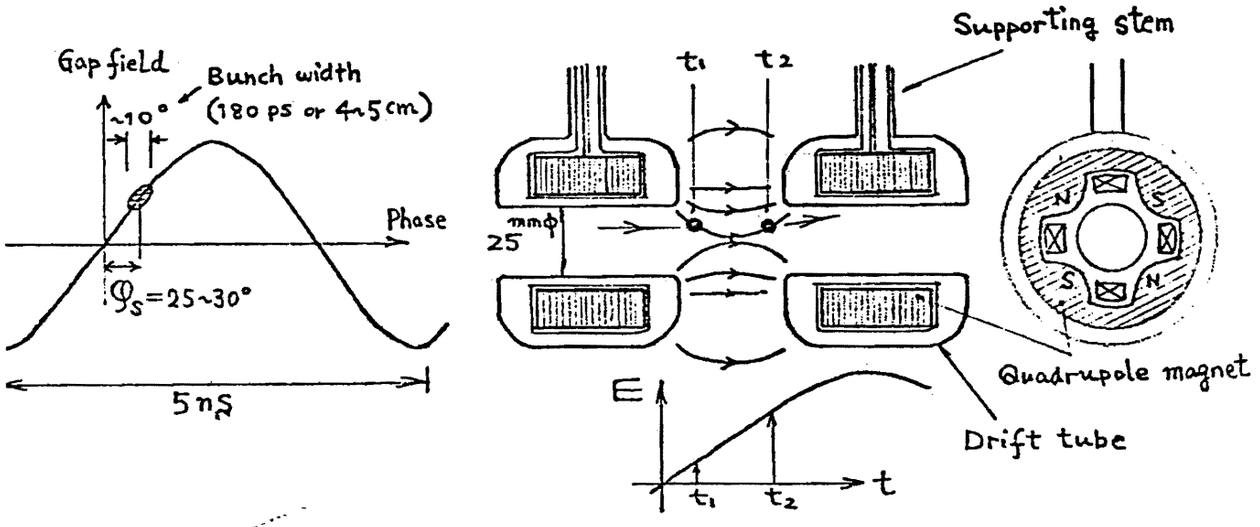

Fig. 13 Phase Focusing and Transverse Defocusing in Linac

Fig. 14 Booster

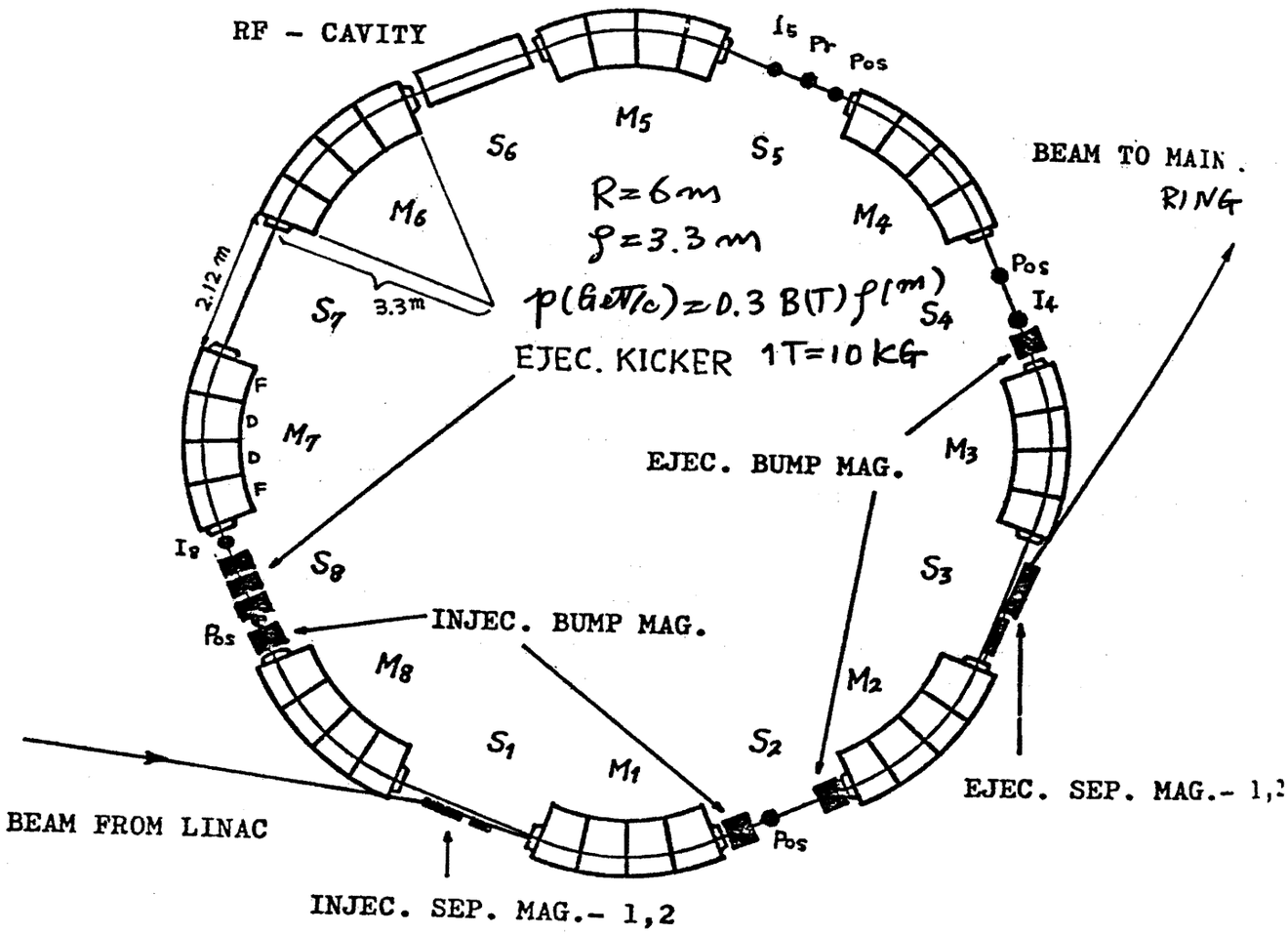

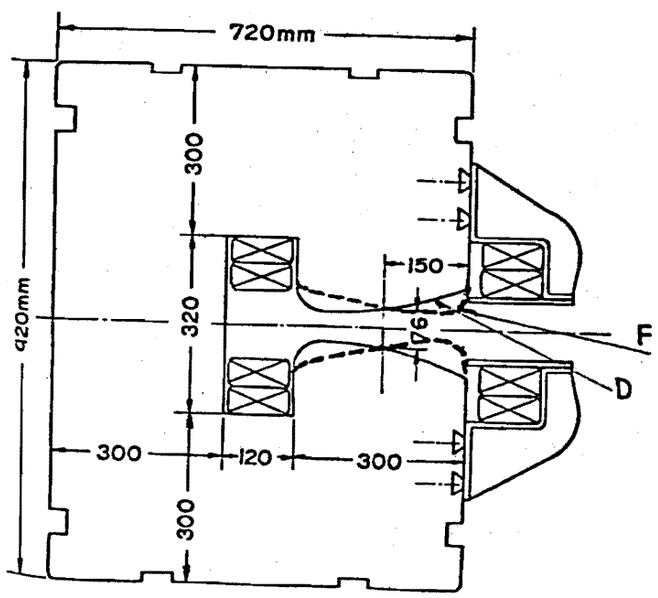

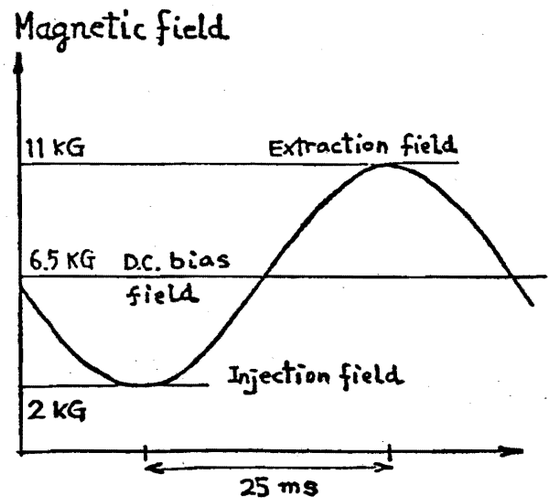

Fig. 15 Cross section of booster magnet ← combined function

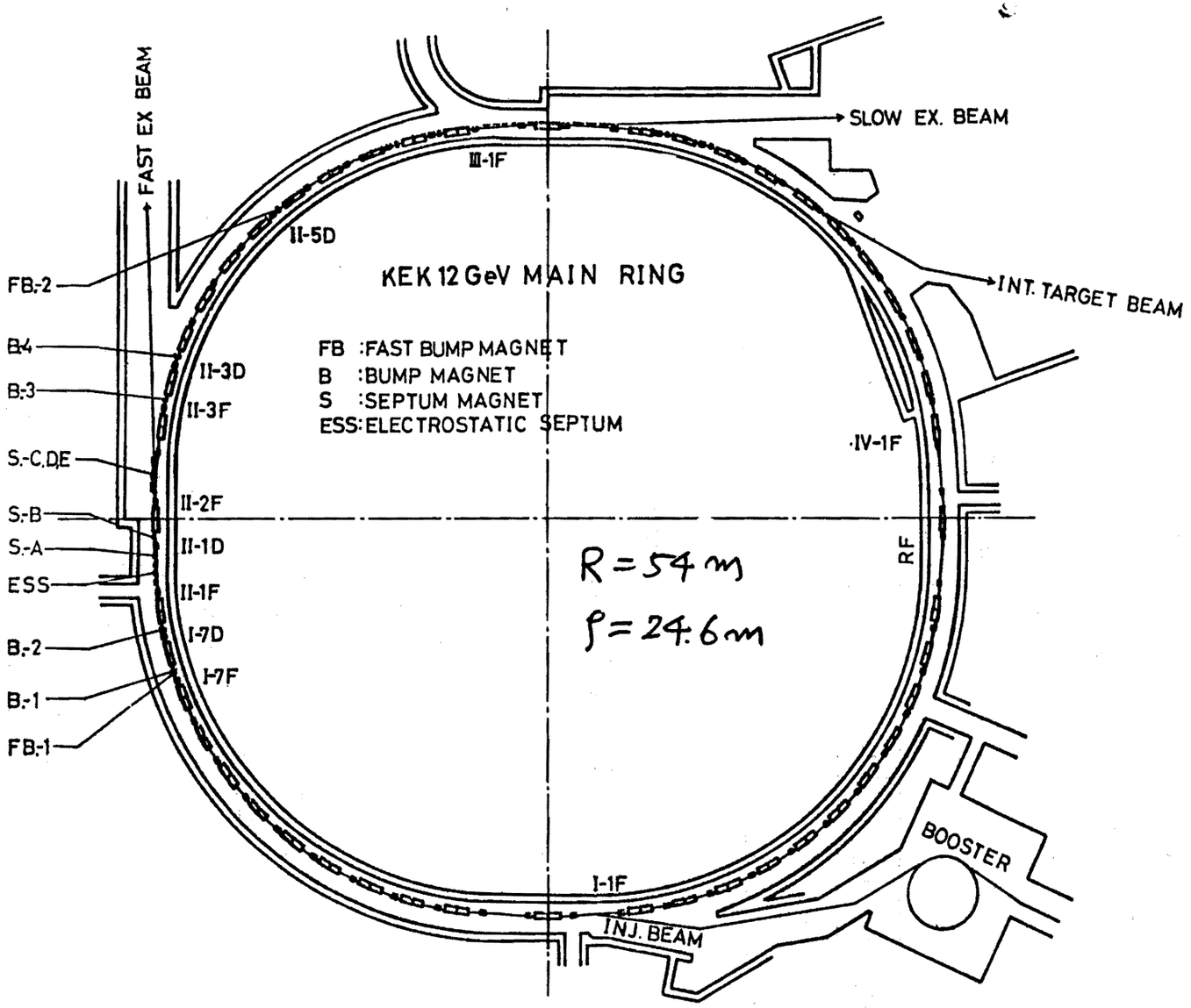

Fig. 16 Main Ring

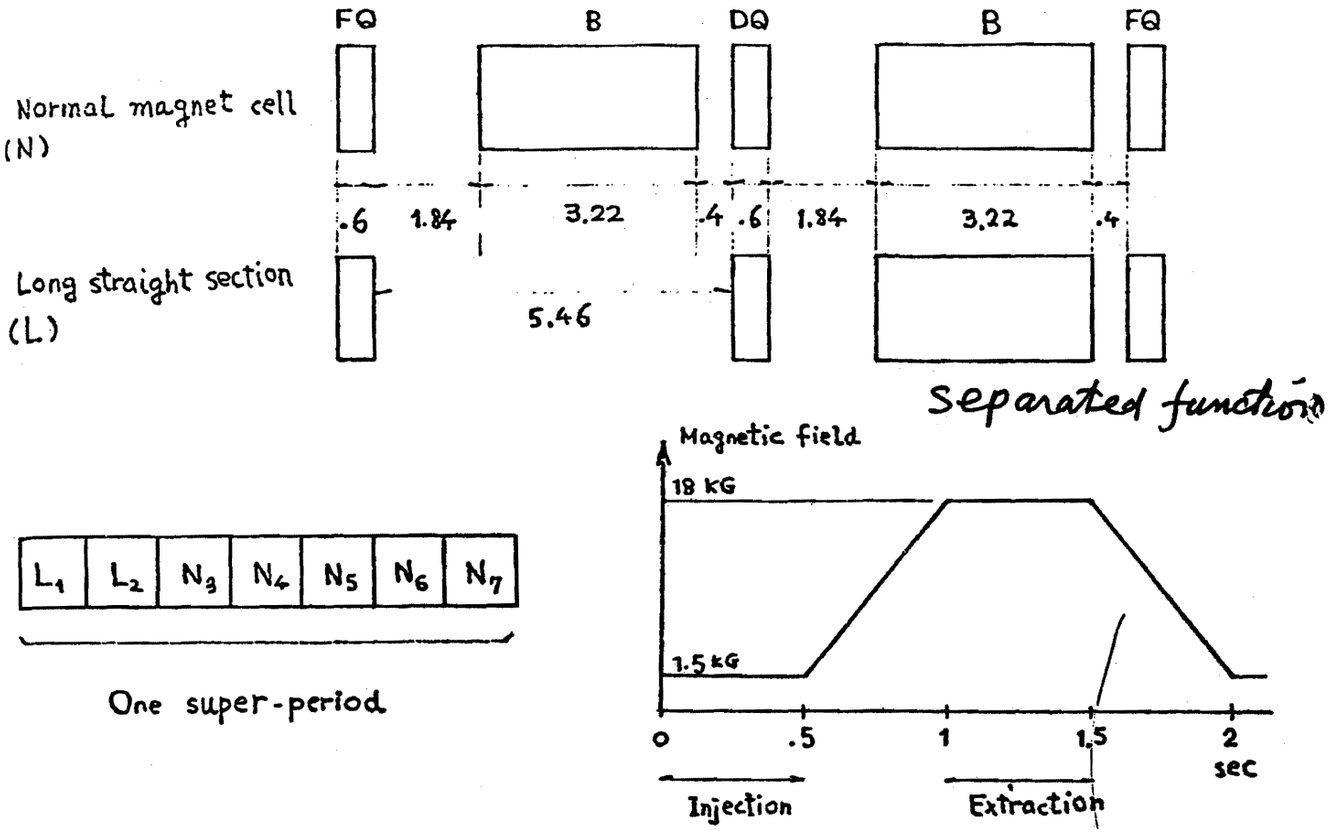

Fig. 17 Structure of Main Ring

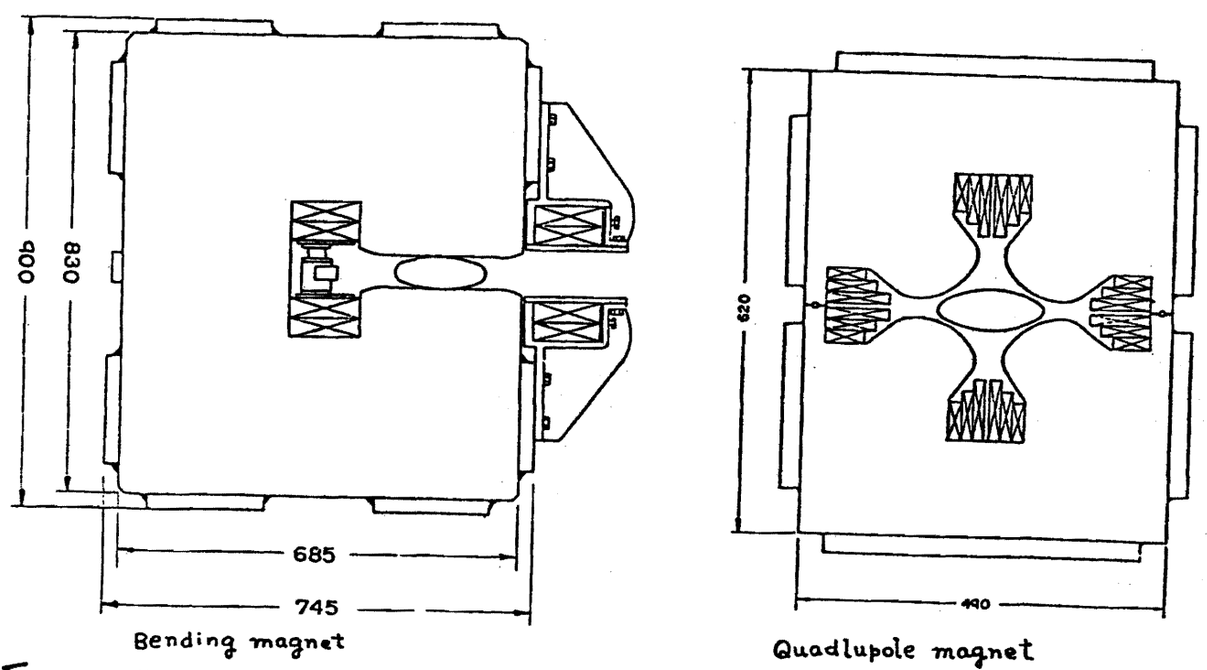

Fig. 18 Cross section of Main ring magnet

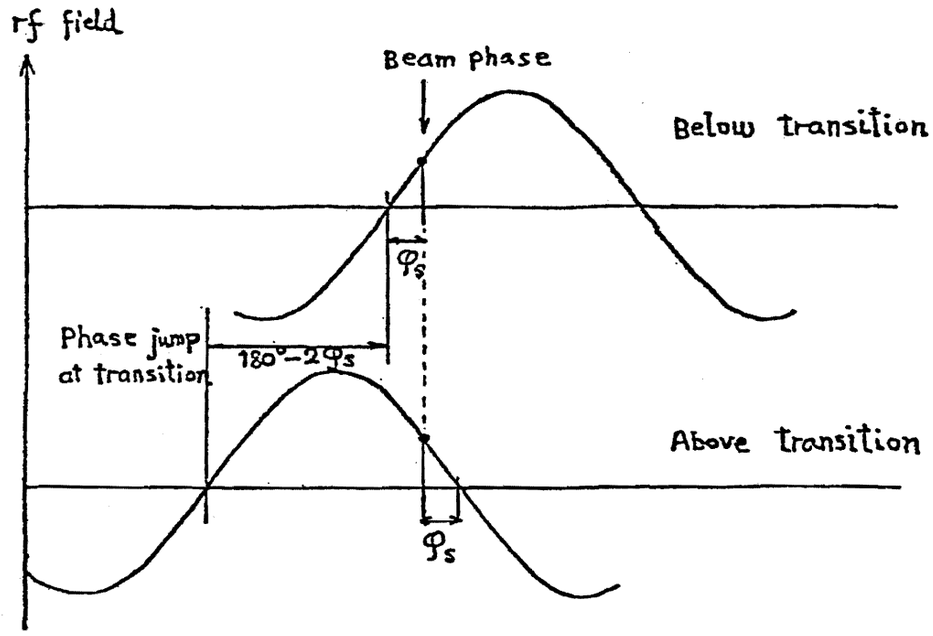

Fig. 19 Phase Stability in Main Ring

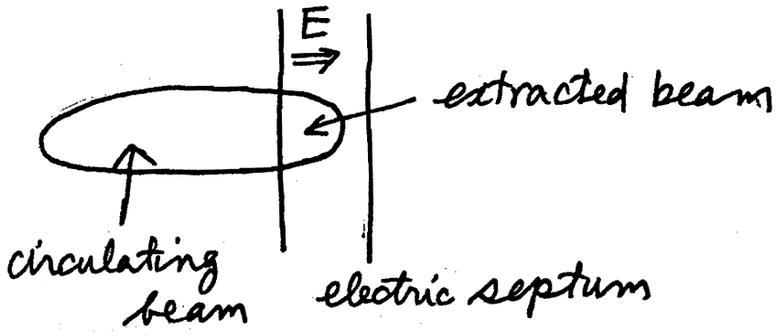

Fast shaving extraction

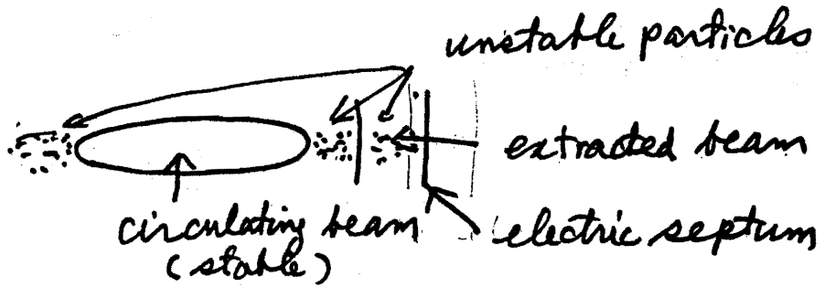

Slow resonant extraction

Fig. 20 Principle of extraction

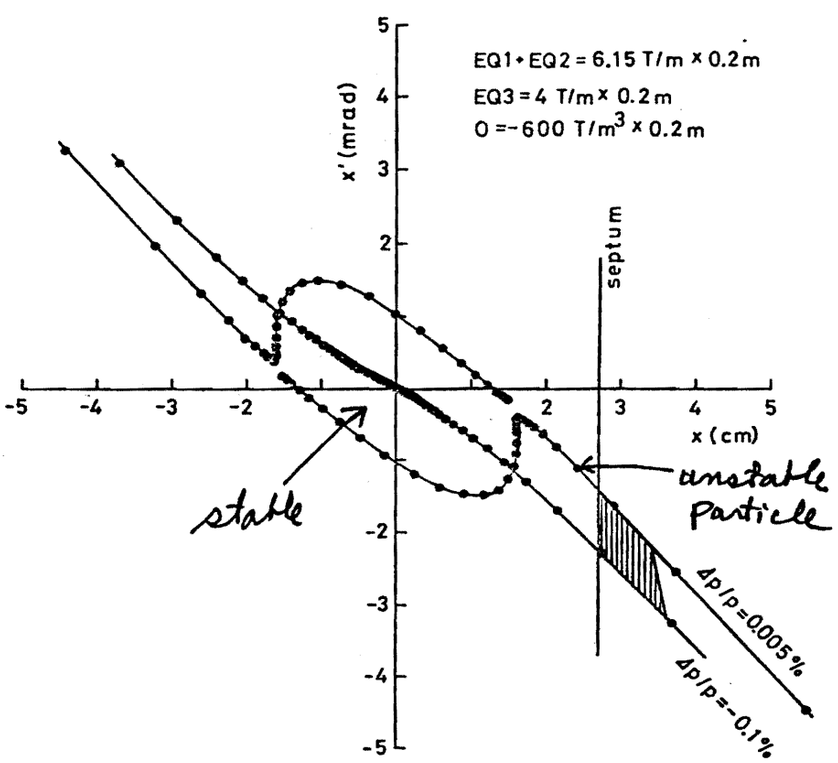

Fig. 21 Stable and Unstable Regions for Slow Extraction

Fig. 22 Synchrotron Radiation

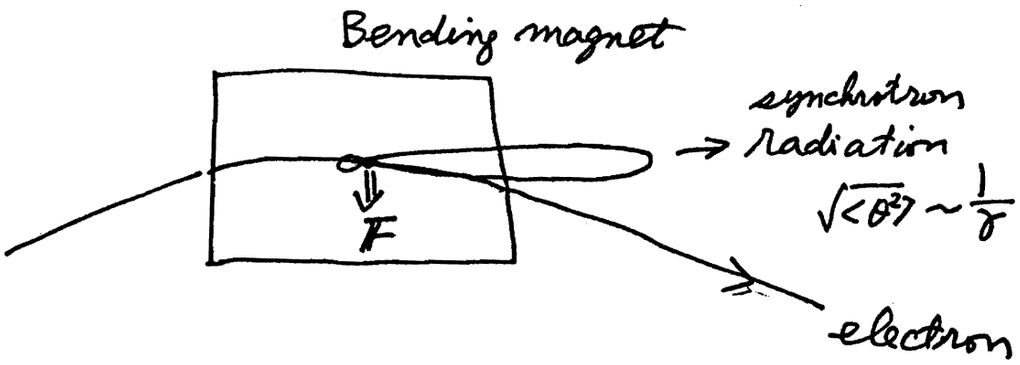

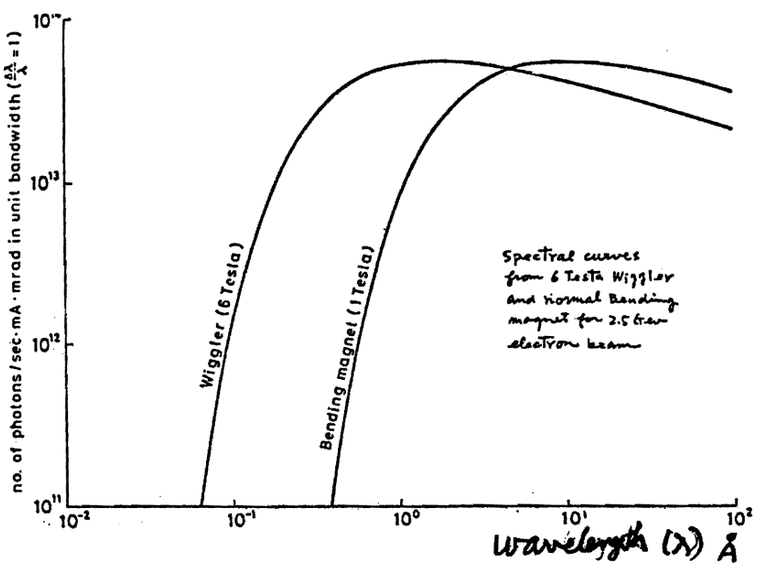

Fig. 23 Spectrum of Synchrotron Radiation

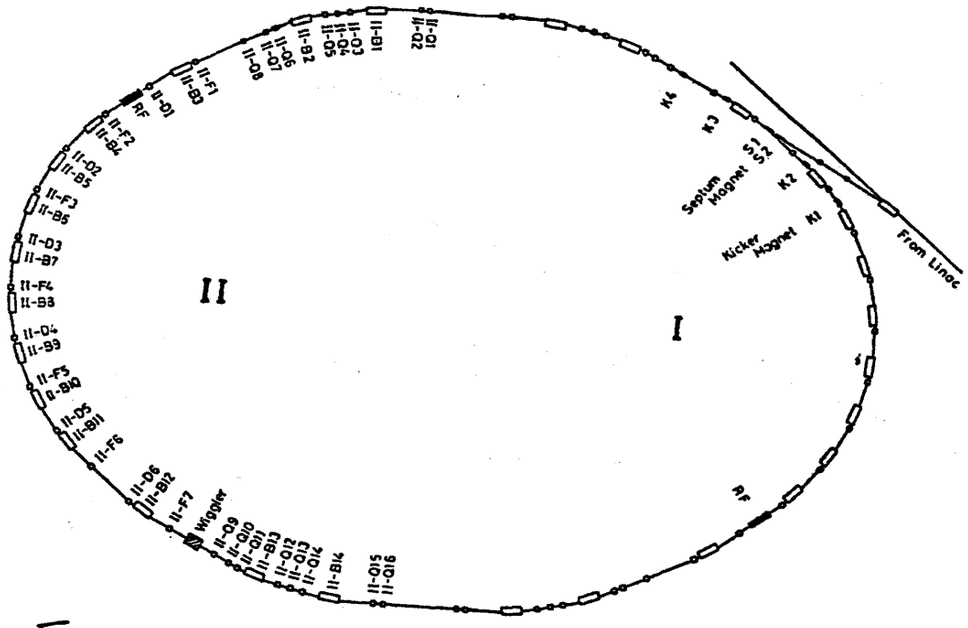

Fig. 24 Photon Factory Storage Ring

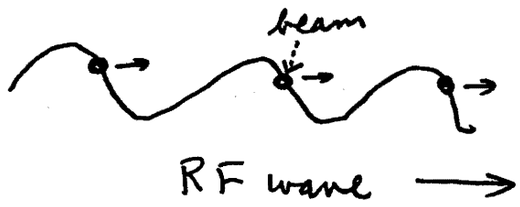

Fig. 25 Principle of a Travelling Wave Type Linac

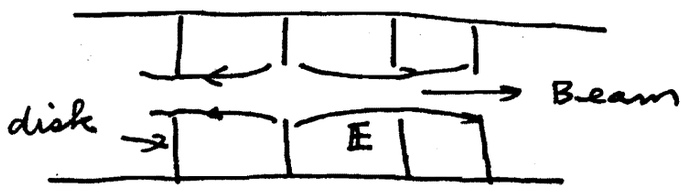

Fig. 26 Slow Wave Structure

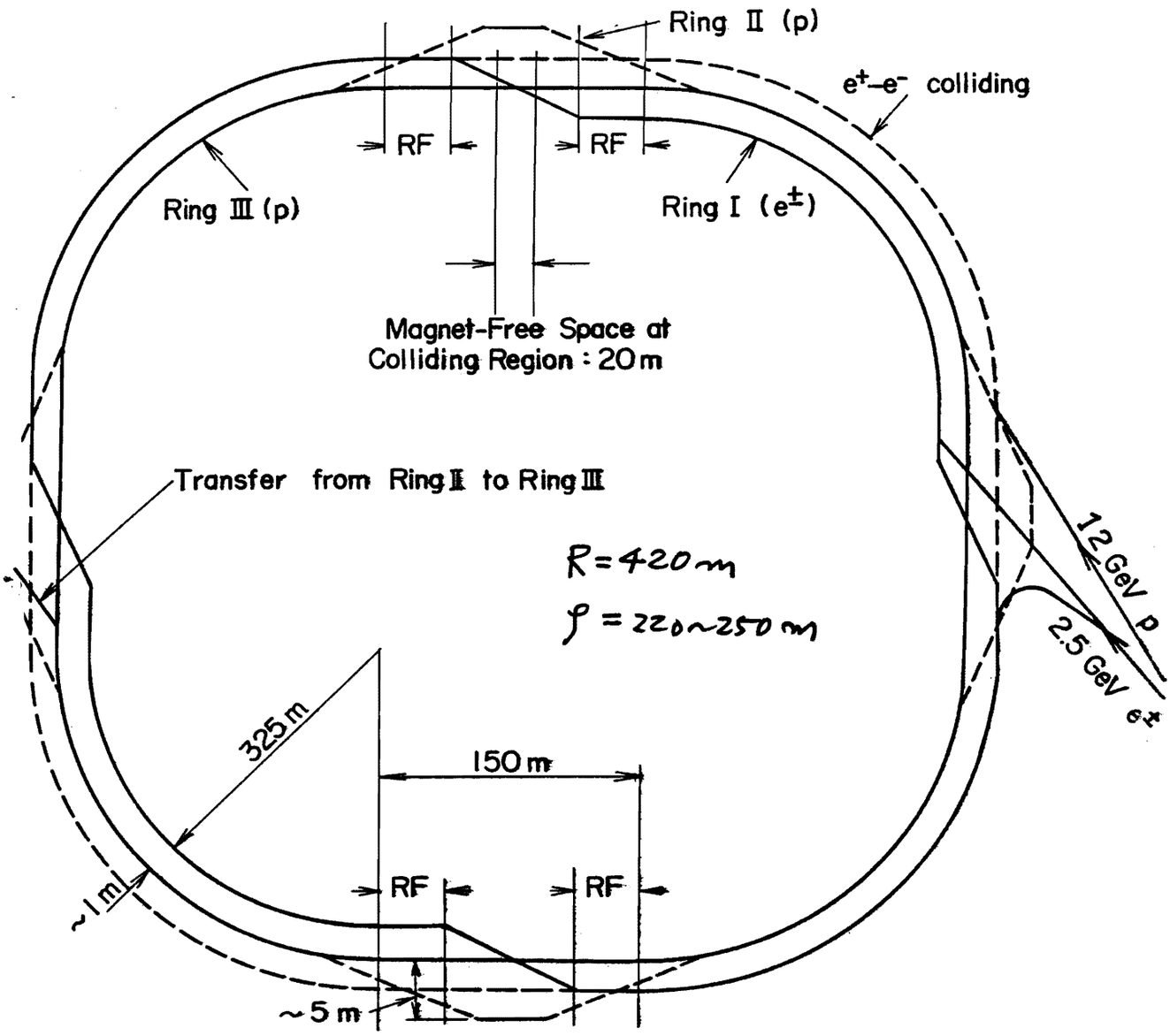

Fig. 27 TRISTAN RINGS